Neutrino-induced meson production in nucleon-decay detectors

T. K. Gaisser
Bartol Research Foundation of the Franklin Institute, University of Delaware, Newark, Delaware 19716

M. Nowakowski and E. A. Paschos
Institut für Physik, Universität Dortmund, 4600 Dortmund 50, West Germany

(Received 8 July 1985)

We give an explicit analytic expression for the angular distribution between lepton and pion in ν-induced charged-current interactions in nuclei. Then we compute the neutrino-induced background including nuclear effects. We find that charge exchange and absorption of the pions within the nuclei are sizable.

I. INTRODUCTION

After a total exposure of several kiloton years, nucleon-decay experiments have accumulated and analyzed more than 300 contained events, most of which are clearly consistent with interactions in the detector of neutrinos produced by cosmic-ray interactions in the atmosphere.[1] The flux of atmospheric ν_μ and ν_e is known from calculations,[2] which have now been checked by these measurements of the rates of interaction of the atmospheric neutrinos.

Among the contained events are some ten candidates for nucleon decay. Since the overall neutrino flux is known, assessing the significance of these candidates now hinges on detailed evaluation of the appearance of ν-induced meson production in the detector. Events of the type

$$\nu+N\rightarrow l+M+N' , \tag{1}$$

in which the recoil nucleon is below threshold for detection can stimulate nucleon decay if the lepton (1) and the meson (M) are sufficiently back-to-back to be consistent with

$$N\rightarrow M+l . \tag{2}$$

The ideal approach to this background problem is to expose each detector to an accelerator neutrino beam with an energy spectrum as close as possible to that of the atmospheric neutrinos. One would need perhaps a factor of ten more statistics for the accelerator exposure than anticipated for the nucleon decay search in order to include rare configurations of neutrino interactions adequately. An alternative approach is to use existing accelerator data obtained with other detectors. In view of the current level of controversy[3] about the estimates of background for nucleon decay, we believe that a third approach, a theoretical calculation of (1), is also of interest. Such a calculation, carried out for various nuclei, could in principle be normalized to a variety of accelerator experiments then used in a uniform way to evaluate backgrounds both in water detectors and in calorimeters containing dense materials. Another advantage of this complementary approach is that there is no statistical limitation to the evaluation of rare configurations.

A full calculation of the background for nucleon decay requires a Monte Carlo treatment of pion production and propagation in the nucleus and in the detector, taking account of Fermi motion and of charge exchange, scattering and absorption of pions both inside and outside the nucleus in which the neutrino interacts. Ultimately, such a complete calculation must be done by each group for its own detector. Our purpose here is to give an expression for the energy and angle distributions of the pions and leptons produced via reaction (1) that can be used as input for a Monte Carlo treatment of propagation. We also illustrate an important nuclear effect; namely, the probability that the direction of the pion is reversed by scattering inside the nucleus. Since pions of interest for proton-decay background ($E_\pi\simeq 470\pm 200$ MeV) are near the region where π-N scattering is dominated by the Δ resonance ($E_\pi\simeq 325\pm 100$ MeV) the intranuclear π-N scattering will be strongly peaked forward and backward. This is evident from the elastic π-N section in the Δ-dominance approximation where

$$\frac{d\sigma}{d\Omega}\propto\sigma_{\pi^+p}(W)(1+3\cos^2\theta) \tag{3}$$

with $W=\sqrt{s}$. Thus there is a substantial probability for a characteristic asymmetric neutrino interaction configuration to be flipped into a back-to-back nucleon-decay configuration and vice versa.

II. NUCLEAR CORRECTIONS

Adler, Nussinov, and Paschos[4] (ANP) calculated nuclear effects on pion production by neutrinos in nuclei taking account of absorption, Pauli effects, and rescattering of pions inside the nucleus (including charge exchange). They have shown that in the region of the (3,3) resonance a forward-backward approximation gives a good description of scattering. For completeness and to define our notation, we outline here the rescattering formalism in the forward-backward approximation. The interested reader can consult ANP for more details.

They describe the scattering as a two-step process. In the first step pions are produced from constituent nu-

cleons of the target nucleus with the free lepton-nucleon cross section. The initial pion multiplicities,

$$\psi_i = \begin{bmatrix} n_i(\pi^+) \\ n_i(\pi^0) \\ n_i(\pi^-) \end{bmatrix}$$

undergo, in the second step, nuclear interaction dependent on the target nucleus and on the kinematic variables. The propagation of the pions is naturally described by the eigenvectors q_k of the charge-exchange matrix M, which has eigenvalues λ_k:

$$q_1 = \begin{bmatrix} 1 \\ 1 \\ 1 \end{bmatrix}, \quad q_2 = \begin{bmatrix} 1 \\ 0 \\ -1 \end{bmatrix}, q_3 = \begin{bmatrix} 1 \\ 2 \\ 1 \end{bmatrix},$$

$$\lambda_1 = 1, \quad \lambda_2 = \tfrac{5}{6}, \text{ and } \lambda_3 = \tfrac{1}{2}.$$

The charge-exchange matrix operates repeatedly on the same vectors and produces a number of emerging pions of charge j denoted by $n_f^+(\pi^j)$. The superscripts + or − indicate pions which emerge without or with a net change in direction, and j is the charge of the pion. The net effect of nuclear rescatterings is summarized by a forward charge-exchange matrix M_+ and a backward matrix M_- as follows:

$$\begin{bmatrix} n_f^{\pm}(\pi^+) \\ n_f^{\pm}(\pi^0) \\ n_f^{\pm}(\pi^-) \end{bmatrix} = M_{\pm} \begin{bmatrix} n_i(\pi^+) \\ n_i(\pi^0) \\ n_i(\pi^-) \end{bmatrix}$$

with

$$M = A \begin{bmatrix} 1-c-d & d & c \\ d & 1-2d & d \\ c & d & 1-c-d \end{bmatrix},$$

where

$$A_{\pm} = g(W,k^2)a_{\pm}, a_{\pm} = f_{\pm}(1),$$

$$d_{\pm} = [1 - f_{\pm}(\tfrac{1}{2})/f_{\pm}(1)]/3$$

and

$$c_{\pm} = \tfrac{1}{3} - \tfrac{1}{2} f_{\pm}(\tfrac{5}{6})/f_{\pm}(1) + \tfrac{1}{6} f_{\pm}(\tfrac{1}{2})/f_{\pm}(1).$$

Here $g(W,k^2)$ is the Pauli factor for pion production by the incident neutrino. A discussion of this and the corresponding factor for suppression of the recoil nucleon in pion-nucleon scattering are to be found in Appendix C of ANP. The factor $f_+(\lambda)$ is the fraction of the eigenfunction q_λ that emerges along the original direction of the neutrino-induced pion and f_- is the fraction that is reversed. The $f_\pm$ depend on the size of the nucleus and on the energy of the pions. Their calculation is described in Appendix A of ANP. Here we compute $f_\pm(\lambda)$ for ^{16}O and give their values as a function of W in Table I.

At each scattering of the pion on its way out of the nucleus there is a chance that it is absorbed. For the absorption cross section we used first an older form

$$\text{(A):} \quad \sigma_{\text{abs}}(W) = \begin{cases} 0, & T < 110 \text{ MeV}, \\ 22 \text{ mb} \times \dfrac{T-110}{290}, & T > 110 \text{ MeV}, \end{cases}$$

where $T = [W^2 - (M_N + m)^2]/(2M_N)$ is the kinetic energy of the pion. More recent measurements of σ_{abs} are accurately represented by[5]

$$\text{(B):} \quad \sigma_{\text{abs}}(W) = \begin{cases} (30 \text{ mb})(T/200 \text{ MeV}), & T < 200 \text{ MeV}, \\ (51.3 \text{ mb})[1 - T/(500 \text{ MeV})], & \\ & 200 < T < 500 \text{ MeV}. \end{cases}$$

For Table I and for all curves and numerical results in this paper we used form (A). In order to study the effect of the new absorption (B) we included in Table II the nuclear effects for both forms (A) and (B), separately. Note that each of these forms represents the absorption cross section per nucleon. Its relation to the total pion absorption cross section per nucleus is discussed by Sparrow.[6]

The formalism of ANP applies to any situation in which a pion originates inside a nucleus, including both nucleon decay and neutrino interactions. In the case of nucleon decay to lepton plus pion, the two decay products start out back-to-back. If the pion backscatters, the event will be effectively removed as a nucleon-decay candidate because the lepton and pion will be nearly colinear. Similarly, a nucleon decay in which the pion is absorbed will also be removed as a candidate. For example, the number

TABLE I. Charge-exchange parameters of ^{16}O for the three eigenvectors as a function of pion-nucleon center-of-mass energy W.

W	$f_+(1)$	$f_+(\frac{5}{6})$	$f_+(\frac{1}{2})$	$f_-(1)$	$f_-(\frac{5}{6})$	$f_-(\frac{1}{2})$
1.10	0.962	0.956	0.944	0.038	0.031	0.018
1.15	0.879	0.850	0.801	0.120	0.093	0.048
1.20	0.691	0.590	0.483	0.216	0.131	0.051
1.25	0.513	0.405	0.322	0.217	0.119	0.045
1.30	0.538	0.487	0.425	0.144	0.099	0.045
1.35	0.540	0.512	0.471	0.093	0.070	0.035
1.40	0.518	0.501	0.473	0.064	0.050	0.026
1.45	0.489	0.477	0.457	0.046	0.036	0.020
1.50	0.459	0.450	0.434	0.035	0.027	0.015

TABLE II. Event rate per kt yr at several stages of the nuclear corrections (see text). F, $0 \le \theta \le 60°$; B, $120° \le \theta \le 180°$.

Reaction	No nuclear corrections F	No nuclear corrections B	With Pauli factor only F	With Pauli factor only B	Pauli factor and charge exchange $F \to B$	Pauli factor and charge exchange $B \to B$	All corrections absorption (A) $F \to B$	All corrections absorption (A) $B \to B$	All corrections absorption (B) $F \to B$	All corrections absorption (B) $B \to B$
$\nu p \to e^- p \pi^+$	0.460	0.288	0.439	0.282	0.76	1.57	0.34	0.66	0.44	0.90
$\nu n \to e^- n \pi^+$	0.051	0.032	0.049	0.031	$\times 10^{-2}$	$\times 10^{-2}$	$\times 10^{-2}$	$\times 10^{-2}$	$\times 10^{-2}$	$\times 10^{-2}$
$\bar{\nu} p \to e^+ n \pi^0$	0.029	0.013	0.027	0.012	0.17	5.14	0.075	3.15	0.10	4.51
$\nu n \to e^- p \pi^0$	0.102	0.064	0.098	0.063	$\times 10^{-2}$	$\times 10^{-2}$	$\times 10^{-2}$	$\times 10^{-2}$	$\times 10^{-2}$	$\times 10^{-2}$
$\bar{\nu} p \to e^+ p \pi^-$	0.014	0.0063	0.013	0.006	0.13	0.36	0.058	0.17	0.07	0.17
$\bar{\nu} n \to e^+ n \pi^-$	0.130	0.057	0.012	0.054	$\times 10^{-2}$	$\times 10^{-2}$	$\times 10^{-2}$	$\times 10^{-2}$	$\times 10^{-2}$	$\times 10^{-2}$

of $p \to e^+ \pi^0$ decays would be reduced by the factor

$$R = f_+(1)(1-2d_+)$$

which can be computed from Table I. For pion kinetic energies in the range 470 ± 200 MeV the pion-nucleon invariant mass is close to the (3,3)-resonance mass and the reduction factor from Table I is approximately $\frac{1}{2}$. This agrees with the calculation of this effect by Sparrow.[6]

III. FORMULAS FOR PRODUCTION VIA Δ RESONANCE

Rein and Sehgal[7] have given a complete treatment of ν-induced pion production in the region of nucleon resonance up to $W=2$ GeV. Their model gives an accurate representation for a large amount of data and agrees with Adler's model[8] in the region of the Δ resonance. For explicit illustration here we show the formulas for Δ(1232), which has the largest production cross section in the region of interest. In the narrow resonance approximation the cross section for

$$\nu + N \to l + \Delta \tag{4}$$

is given by

$$\frac{d\sigma_\nu}{dE_l}(\bar{\nu}) = 2m \left[\frac{d\sigma_A}{dq^2} \pm \frac{d\sigma_{VA}}{dq^2} + \frac{d\sigma_V}{dq^2} \right] , \tag{5}$$

where

$$\frac{d\sigma_A}{dq^2} = \frac{G_F^2}{32\pi} \frac{(\Delta+m)^2}{m^2 Q^2} [2uv(\Delta-m)^2 + (-q^2)(u^2+v^2)] G_A^2 ,$$

$$\frac{d\sigma_V}{dq^2} = \frac{2G_F^2}{\pi}(u^2+v^2) \frac{(-q^2)(\Delta+m)^2}{[(\Delta+m)^2-q^2]^2} G_V^2 ,$$

and

$$\frac{d\sigma_{VA}}{dq^2} = \frac{G_F^2}{2\pi}(u^2-v^2) \frac{(-q^2)}{mQ} \frac{(\Delta+m)^2}{(\Delta+m)^2-q^2} G_V G_A .$$

The notation here is that of Rein and Sehgal,[7] with

$$G_{V(A)}(q^2) = \frac{1}{(1-q^2/m_{V(A)}^2)^2} ,$$

$q_\mu = (E_\nu - E_1, \mathbf{Q})$ is the four-momentum transfer, $\Delta = 1.23$ GeV, and $u(v) = (E_\nu + E_1 \pm Q)/2E_\nu$, $m_V = 0.84$ GeV, and $m_A = 0.95$ GeV. Since $q^2 + 2m(E_\nu - E_1) + m^2 = W^2$ and $W^2 \to \Delta^2$ in the narrow-resonance approximation, the cross section depends only on E_ν and E_1 in this approximation with the laboratory four-momentum of the resonance given by

$$p_\mu^\Delta = (E_\nu + m - E_1', \mathbf{Q}) . \tag{6}$$

Then assuming isotropic decay in the Δ rest frame leads to a uniform distribution in pion laboratory energy with

$$E_\pi = \gamma E^* + \beta\gamma p^* \cos\theta^* , \tag{7}$$

where $E^* \simeq 0.264$ GeV, $p^* \simeq 0.224$ GeV, and θ^* are, respectively, the pion energy, momentum, and angle relative to the Δ direction in the rest frame of the Δ, and the Lorentz factors are calculated from Eq. (6). Thus we can write the normalized cross section for the contribution of the Δ to reaction (1) as

$$\frac{d\sigma(E_\nu)}{dE_l dE_\pi d\phi} = \frac{1}{4\pi\beta\gamma p^*} \frac{d\sigma(E_\nu)}{dE_l} , \tag{8}$$

where ϕ is the (unmeasurable) azimuthal angle of the pion relative to the 1–Δ plane. The measurable angular quantity is $\theta_{\pi l} \equiv \theta$. Changing angular variables gives

$$\frac{d\sigma(E_\nu)}{dE_l dE_\pi d\cos\theta} = \frac{1}{2\pi\beta\gamma p^*} \frac{d\sigma}{dE_l} \frac{\left[1 - \left[\dfrac{\cos\theta - \cos\theta_1\cos\theta_2}{\sin\theta_1\sin\theta_2}\right]^2\right]^{-1/2}}{\sin\theta_1\sin\theta_2} , \tag{9}$$

where $\theta_1 \equiv \theta_{\pi\Delta}$ and $\theta_2 \equiv \theta_{l\Delta}$ are determined by kinematics in terms of E_l, E_π, and the resonance mass. Equations (8) and (9) are valid for any resonance in the narrow-resonance approximation when the appropriate $d\sigma/dE_1$ is used.

To obtain a physically meaningful result Eq. (9) must be folded with the neutrino flux. We use for the fluxes[2] (using as units $\text{cm}^{-2}\,\text{s}^{-1}\,\text{sr}^{-1}\,\text{GeV}^{-1}$)

$$\frac{dI(\nu_\mu + \bar{\nu}_\mu)}{dE_\nu} = \frac{0.069}{(E_\nu + 0.30\ \text{GeV})^3} , \tag{10}$$

$$\frac{dI(\nu_e+\bar{\nu}_e)}{dE_\nu}=\frac{0.031}{(E_\nu+0.30\ \text{GeV})^3}\left[\frac{20}{20+E_\nu}\right], \quad (11)$$

and for the ratios we take $\nu/\bar{\nu}=1.2$ for both ν_e and ν_μ. The integrated flux for the sum of all types of neutrinos with $E_\nu > 1$ GeV is

$$\int_1^\infty I_\nu(E)dE = 2.98\times10^{-2}\ \text{cm}^{-2}\text{s}^{-1}\text{sr}^{-1}\ . \quad (12)$$

As a check on the formalism we first compute several quantities for the process

$$\bar{\nu}_e+p\rightarrow e^+ +\pi^0+n \quad (13)$$

and compare with the result of Rein.[9] Figure 1 shows the angular distribution $d\sigma/d\theta_{e\pi}$ for reaction (13), integrated over the atmospheric neutrino spectrum and with M_N-200 MeV $< E_l+E_\pi < M_N+200$ MeV. The shape is very close to the distribution of Rein.

We next compute the total number of events expected for reaction (13) alone with $\theta_{e\pi} > 120°$, subject to the above energy cuts and integrated over the neutrino spectrum. (This is the integral of Fig. 1 from 120° to 180°.) We find $N(e^+\pi^0)=1.26\times10^{-2}$ events per kiloton year (kt yr) which is a factor 2.7 smaller than the value of Rein.[9] Since the spectra for $E_{\bar{\nu}_e} > 1$ GeV are essentially the same, we must attribute[10] the difference to the flux-averaged cross section for $E_{\bar{\nu}_e} < 1$ GeV.

IV. BACKGROUND FOR $p\rightarrow e^+\pi^0$

Finally we must include all the nuclear effects of Sec. II to obtain the contribution from all channels to the background for this decay mode. Because of charge exchange and the fact that the detectors cannot distinguish electrons from positrons, this will include contributions from pions of all charges and from neutrinos as well as antineutrinos. The latter is particularly important since the neutrino cross section is substantially larger than that of the antineutrino in the GeV region.

Figure 2 shows the angular distributions with and without nuclear corrections (dashed and solid curves, respectively). The six relevant processes are listed in Eq. (14):

$$\nu_e+p\rightarrow e^-+\pi^+ +p\ , \quad (14a)$$

$$\nu_e+n\rightarrow e^-+\pi^0+p\ , \quad (14b)$$

$$\nu_e+n\rightarrow e^-+\pi^+ +n\ , \quad (14c)$$

$$\bar{\nu}_e+p\rightarrow e^+ +\pi^0+n\ , \quad (14d)$$

$$\bar{\nu}_e+p\rightarrow e^+ +\pi^- +p\ , \quad (14e)$$

$$\bar{\nu}_e+n\rightarrow e^+ +\pi^- +n\ . \quad (14f)$$

Before nuclear corrections are included only (14b) and (14d) contribute to the background for proton decay to electron and neutral pion. When charge exchange is included all six channels contribute. Thus the solid curve in Fig. 2 is the angular distribution for processes (14b) + (14d). The dashed curve includes contributions from all channels after all corrections have been applied.

In order to understand the origin of the nuclear effects we summarize in Table II some intermediate steps in the calculation. Columns 2 and 3 give the the numbers of events per kt yr for each channel integrated over the angular regions $0<\theta<60°$ and $120°<\theta<180°$, respectively. The next step is to add the nuclear corrections one by one. Columns 4 and 5 show the effect of the Pauli factor. Columns 6 and 7 include charge exchange without absorption. The last columns summarize the net contribution of each channel to the $e\pi^0$ final state, including absorption

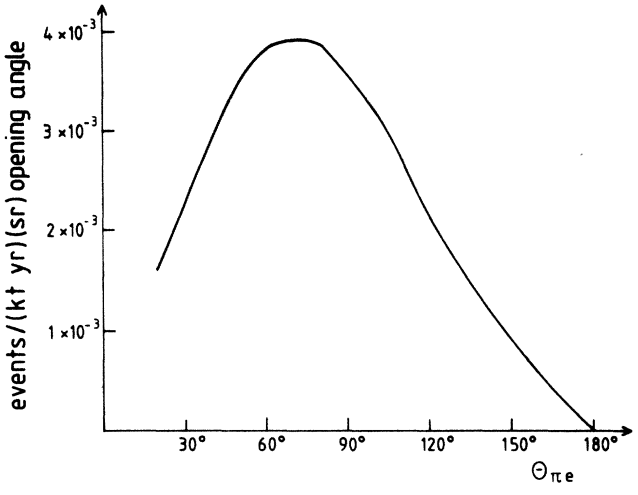

FIG. 1. Distribution of laboratory opening angle between π^0 and e^+ induced by atmospheric electron antineutrinos subject to the cuts described in the text and integrated over the antineutrino energy spectrum. In all figures the events are given per solid angle of the incident neutrinos or antineutrinos and per opening angle in radians.

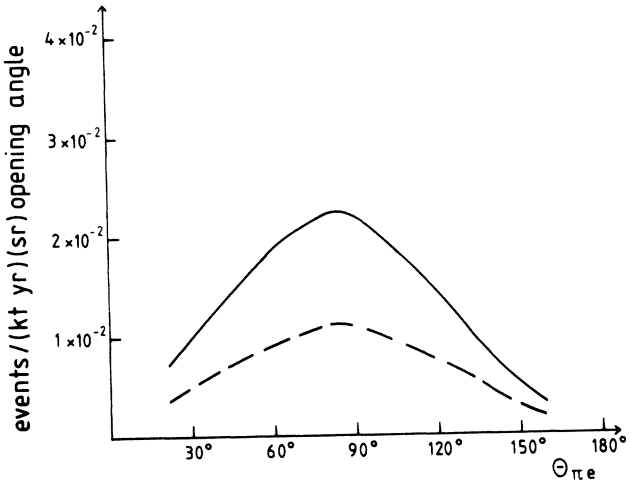

FIG. 2. Distribution of the laboratory opening angle between π^0 and the lepton induced by atmospheric neutrinos and antineutrinos (together) integrated over the neutrino and antineutrino spectra. The solid curve is the sum of processes (14b) and (14d) without nuclear corrections. The dashed curve is with nuclear corrections, and all channels in Eq. (14) contribute. The same units are used as in Fig. 1.

in the nucleus. Columns 8 and 9 are with absorption (A) and columns 10 and 11 with absorption (B). Because of backscattering both columns 2 and 3 contribute to the final rate of events with electron-pion opening angle greater than 120°. The total background for $p \to e^+ + \pi^0$ is the sum of the entries in columns 8 and 9 [for absorption (A)] or columns 10 and 11 [absorption (B)]. Rescattering enhances the background since the large $\pi^+ p$ channel feeds into the $e\pi^0$ channel. With the more realistic absorption (B), the total calculated background is 6×10^{-2} events/kt yr. In practice, the total background for this decay mode must also include nuclear rescattering and absorption of pions in nuclei outside the nucleus in which the pion originates. The size of this correction will depend on the vertex resolution of each detector and must be done separately for each experiment, but it will increase the background.

Finally, in Fig. 3 we display the dependence of the results on energies of leptons and pions. In each case the solid lines show the results without and the dashed curves with nuclear corrections. The upper pair of curves includes lepton-pion opening angles from 120° to 180° and the lower pair from 150° to 180°. The results are weighted by the neutrino/antineutrino fluxes and are doubly differential in lepton and pion energies.

In most instances nuclear corrections lower the double

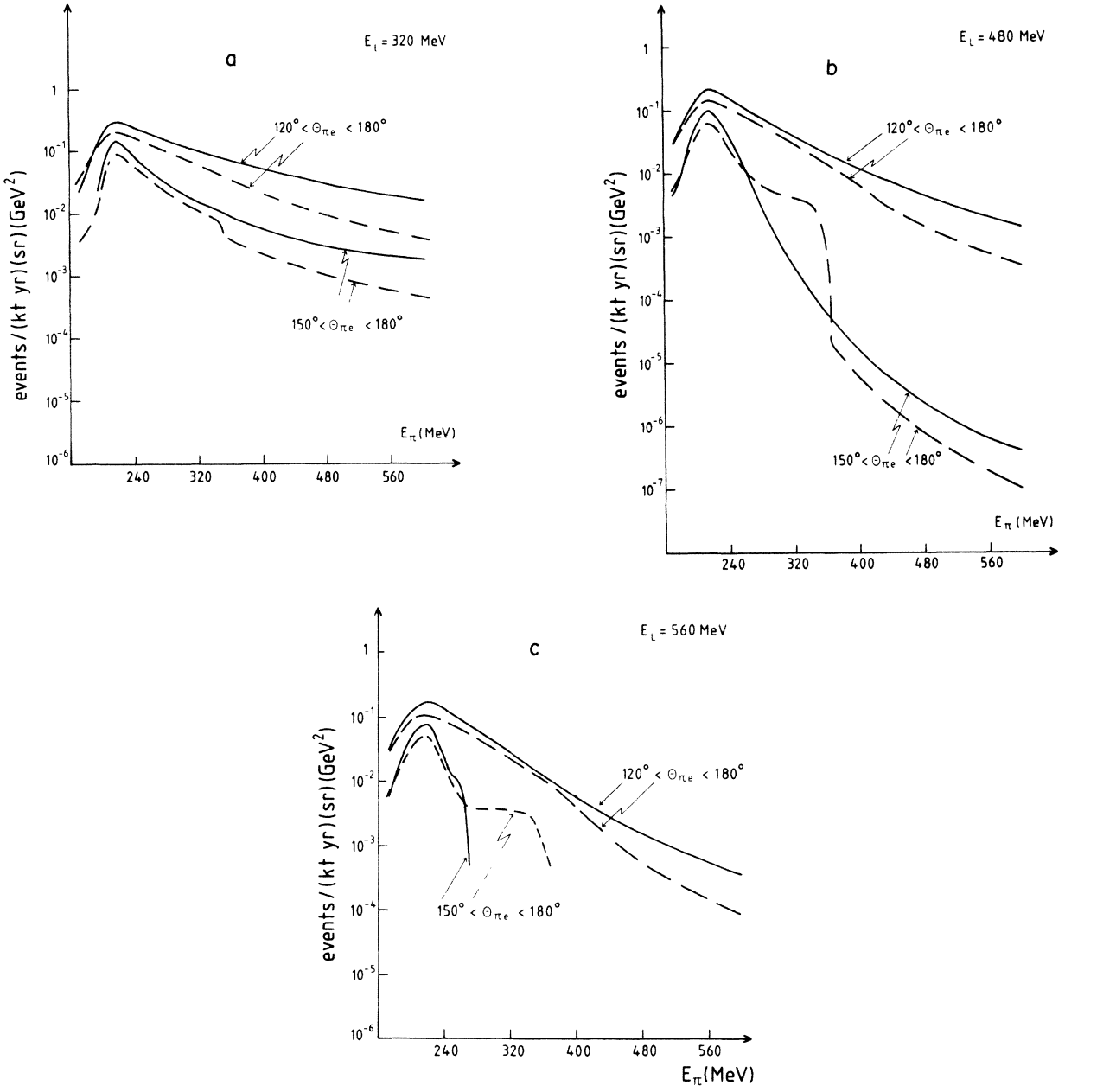

FIG. 3. (a) Number of events produced by atmospheric neutrinos and antineutrinos as a function of lepton (E_l) and pion (E_π) energies. Solid curves are without nuclear corrections and dashed curves with. (b) Same as (a) with $E_l = 480$ MeV. (c) Same as (a) with $E_l = 560$ MeV.

differential cross sections of Fig. 3; in some cases there are steplike decreases. In Fig. 3(a), this happens at $E_\pi = 320$ MeV for the topology $150° \leq \theta_{\pi e} \leq 180°$, when one runs out of phase space and there are no more forward events to be flipped into the backward direction. There are also two other cases of interest. First, in Fig. 3(b) appears a region where the curve with nuclear corrections is larger than the solid curve. At these energies there are more events from the $f \rightarrow b$ transition than those which maintain their backward direction. Its origin lies in the flux averaging where for a given set of energies (E_π, E_l) one needs higher neutrino energies to induce a back-to-back reaction than for the forward reaction. Thus there is a large number of events where the pions backscatter and become proton-decay candidates. The second case occurs in Fig. 3(c) for the $150° \leq \theta_{\pi e} < 180°$ topology. The curve without nuclear corrections runs out of phase space for $E_\pi \geq 280$ MeV, while the dashed curves extend further; these are again forward events where the pions scattered backward.

V. DISCUSSION

Estimates of the background for $p \rightarrow e\pi^0$ in water detectors based on previous neutrino experiments are in the range 0.03–0.2 events per kiloton year.[11] Our result from Table II of 0.06 events per kiloton year is in reasonable agreement with this. We note that our calculation does not include contributions from scattering in nuclei in the surrounding medium.

In the future it will be of interest to carry out similar background calculations in iron in order to be able to compare expected background rates in dense detectors with those in water detectors. Also it will be useful to use results of the present calculation as the input for various detector Monte Carlo models. This would provide alternate background estimates to the present ones based on Gargamelle and other neutrino experiments that were not originally designed for this purpose.

ACKNOWLEDGMENTS

Two of us (M.N. and E.A.P.) wish to thank Dr. D. Rein and Dr. L. M. Sehgal for discussions and correspondence concerning their work and Dr. D. P. Roy for help with the computing programs and his interest in this work. T.K.G. is grateful to J. M. Lo Secco, A. K. Mann, and A. Suzuki for helpful discussions. The work of T.K.G. was supported in part by the U.S. Department of Energy. The work of E.A.P. was supported in part by a grant of the German Bundesministerium für Forschung und Technologie.

[1]D. H. Perkins, in *Neutrino '84*, proceedings of the 11th International Conference on Neutrino Physics and Astrophysics, Dortmund, 1984, edited by K. Kleinknecht and E. A. Paschos (World Scientific, Singapore, 1984), pp. 374 and 331–370.

[2]T. K. Gaisser and Todor Stanev, in *Neutrino '84* (Ref. 1), p. 370. The specific approximations used in Eqs. (10) and (11) are based on fluxes at Kamioka, and are valid only for neutrino energies above 0.7 GeV, which is relevant for Δ production.

[3]T. W. Jones, in *Neutrino '84* (Ref. 1), p. 331; S. Miyake, in *Neutrino '84* (Ref. 1), p. 344; O. Saavedra, in *Neutrino '84* (Ref. 1), p. 350; M. L. Marshak, in *Neutrino '84* (Ref. 1), p. 362.

[4]S. L. Adler, S. Nussinov, and E. A. Paschos, Phys. Rev. D **9**, 2125 (1974).

[5]R. R. Silbar and M. M. Sternheim, Phys. Rev. C **8**, 492 (1973).

[6]D. A. Sparrow, Phys. Rev. Lett. **44**, 625 (1980).

[7]D. Rein and L. M. Seghal, Ann. Phys. (N.Y.) **133**, 79 (1981).

[8]S. L. Adler, Ann. Phys. (N.Y.) **50**, 89 (1968).

[9]D. Rein, Phys. Rev. D **28**, 1800 (1983); **30**, 242(E) (1984).

[10]In the meanwhile Rein has run his programs with the fluxes in Eqs. (10) and (11) and verified this result (private communication).

[11]H. S. Park *et al.*, Phys. Rev. Lett. **54**, 22 (1985); J. M. LoSecco (private communication).